

PAPER • OPEN ACCESS

Extracting work from coherence in a two-mode Bose–Einstein condensate

To cite this article: L A Williamson *et al* 2025 *Quantum Sci. Technol.* **10** 015040

View the [article online](#) for updates and enhancements.

You may also like

- [OnionVQE optimization strategy for ground state preparation on NISQ devices](#)
Katerina Gratsea, Johannes Selisko, Maximilian Amsler et al.
- [Angular Bloch oscillations and their applications](#)
Bernd Konrad and Maxim Efremov
- [Quantum Onsager relations](#)
Mankei Tsang

Quantum Science and Technology



PAPER

Extracting work from coherence in a two-mode Bose–Einstein condensate

OPEN ACCESS

RECEIVED
11 July 2024

REVISED
18 October 2024

ACCEPTED FOR PUBLICATION
7 November 2024

PUBLISHED
29 November 2024

Original Content from
this work may be used
under the terms of the
[Creative Commons
Attribution 4.0 licence](#).

Any further distribution
of this work must
maintain attribution to
the author(s) and the title
of the work, journal
citation and DOI.



L A Williamson^{1,*} , F Cerisola² , J Anders^{2,3}  and Matthew J Davis^{1,*} 

¹ ARC Centre of Excellence for Engineered Quantum Systems, School of Mathematics and Physics, University of Queensland, St Lucia, Queensland 4072, Australia

² Department of Physics and Astronomy, University of Exeter, Stocker Road, Exeter EX4 4QL, United Kingdom

³ Institut für Physik und Astronomie, University of Potsdam, 14476 Potsdam, Germany

* Authors to whom any correspondence should be addressed.

E-mail: lewis.williamson@uq.edu.au and mdavis@uq.edu.au

Keywords: work, coherence, Bose–Einstein condensate, resource, thermodynamics

Abstract

We show how work can be extracted from number-state coherence in a two-mode Bose–Einstein condensate. With careful tuning of parameters, a sequence of thermodynamically reversible steps transforms a Glauber coherent state into a thermal state with the same energy probability distribution. The work extracted during this process arises entirely from the removal of quantum coherence. More generally, we characterise quantum (from coherence) and classical (remaining) contributions to work output, and find that in this system the quantum contribution can be dominant over a broad range of parameters. The proportion of quantum work output can be further enhanced by squeezing the initial state. Due to the many-body nature of the system, the work from coherence can equivalently be understood as work from entanglement.

1. Introduction

Converting disordered energy (heat) into ordered energy (work) is one of the most fundamental processes in thermodynamics. In a classical system, disorder arises from practical limitations on what can be known about a large system. Observables in a quantum system may exhibit not only classical uncertainty, but also quantum uncertainty arising from coherence [1, 2]. Quantum coherence is defined with respect to a particular basis, and occurs when a system exists in superpositions of eigenstates of that basis. Of particular relevance to thermodynamics is the quantum uncertainty in a system's energy, arising from coherence in the energy eigenbasis [3–5].

It is now well established that coherence in the energy eigenbasis can enhance work extraction if appropriately utilised. For a sufficiently rapid engine cycle, coherence can enhance power output beyond that of any classical engine operating with the same resources [6–8]. In single-shot realisations, coherence may diminish the maximum available work [9], however, a carefully chosen sequence of thermodynamic processes circumvents this degradation [10–13]. Despite the benefits of coherence in work extraction, protocols to realise these benefits in experimentally tractable systems are lacking. Such expositions are timely, considering the relevance to quantum information [14–16] and the growing field of quantum thermal machines [17, 18].

Bose–Einstein condensates (BECs) offer a pristine system in which to explore many-body quantum physics, due to a high degree of tuneability and isolation from the environment [19, 20]. In the field of quantum thermal machines, bosonic particle statistics can improve engine performance [21–24] and act as a fuel in an engine-like cycle [25]. Interactions in a BEC can enhance engine performance [26, 27] or allow access to energetic degrees of freedom not available classically [28, 29]. However, the role of coherence in work extraction from a BEC has not been explored. Notably, two-mode BECs can exhibit long-lived coherence in the number state basis [30]. Incorporating squeezing [31–33], two-mode BECs can exhibit metrologically useful entanglement, allowing for quantum-enhanced measurement sensitivity [34–36].

In this manuscript we show how number-state coherence in a two-mode BEC can empower work extraction. To obtain work that is predominantly quantum in origin the initial state must be close to thermal

when projected onto the energy eigenbasis. This is challenging in a quantum many-body system due to the exponentially large number of populations and coherences. We show that this challenge can be overcome by using a Glauber coherent state (GCS) with mean boson number less than a critical value that depends on temperature. We introduce a formalism to quantify the work directly available from coherence and the work that would be available classically, and show that squeezing the initial state can substantially increase the proportion of quantum work extracted. The number-state coherence in our protocol arises from entangling correlations between the two modes of the BEC. Therefore the work extracted from coherence can equivalently be interpreted as work from entanglement, thus demonstrating the many-body nature of the protocol. To our knowledge, our work presents the first proposal showing how work can be extracted from coherence in a two-mode BEC, paving the way for experimental demonstration and highlighting the utility of two-mode BECs in thermodynamic applications.

2. Background

2.1. Extracting work from coherence

To see how work can be extracted from quantum coherence generally, consider a Hamiltonian \hat{H} with thermal state $\rho_{\text{therm}} = e^{-\beta\hat{H}} / \text{Tr} e^{-\beta\hat{H}}$ at inverse temperature β . Now consider a second quantum state ρ that satisfies

$$\langle E_n | \rho | E_n \rangle = \langle E_n | \rho_{\text{therm}} | E_n \rangle, \quad (1)$$

with $|E_n\rangle$ the energy eigenstates of \hat{H} . The information entropy associated with energy measurements of state ρ (termed ‘energy entropy’ in [5]) is

$$S^E = - \sum_n \langle E_n | \rho | E_n \rangle \ln \langle E_n | \rho | E_n \rangle, \quad (2)$$

which for an isolated system is non-decreasing under time evolution [37, 38]. When equation (1) is satisfied, the energy entropy of state ρ is identical to that of ρ_{therm} . If ρ is diagonal in the energy eigenbasis then S^E is equal to the von Neumann entropy $S^V = -\text{Tr}[\rho \ln \rho]$ and ρ is equal to ρ_{therm} , which is a completely passive state [39]. If, however, ρ contains coherences (off-diagonal) terms in the energy eigenbasis, S^E will differ from S^V [37, 40, 41]. The difference between the two,

$$S^E - S^V = \sum_{m,n \neq m} \langle E_m | \rho | E_n \rangle \langle E_n | \ln \rho | E_m \rangle, \quad (3)$$

can be extracted in the form of non-classical work [11, 13, 42]

$$W_{\text{quant}} = \beta^{-1} (S^E - S^V) = \beta^{-1} D(\rho || \rho_{\text{ed}}). \quad (4)$$

Here $D(\rho || \sigma) = \text{tr}[\rho \ln \rho] - \text{tr}[\rho \ln \sigma] \geq 0$ is the quantum relative entropy, and $\rho_{\text{ed}} = \sum_n \langle E_n | \rho | E_n \rangle |E_n\rangle \langle E_n|$ is the *projection* of the density matrix ρ onto the energy eigenstates (the ‘energy diagonal’ density matrix). The quantity $D(\rho || \rho_{\text{ed}})$ is a monotonic measure of the quantum coherence of state ρ [43] and hence the work output, equation (4), is quantum in origin.

A protocol to extract work from coherence was presented in [11]. The efficacy of this protocol depends on how closely the system’s mean energy and energy entropy match that of the thermal state ρ_{therm} . When these match, any work extracted during the protocol is entirely from coherence. A sufficient condition for this matching is that $\rho_{\text{ed}} = \rho_{\text{therm}}$, equation (1). This can always be satisfied in a two-level system by choosing the temperature of ρ_{therm} to satisfy [44]

$$k_B T = \frac{E_1 - E_0}{\ln \frac{\langle E_0 | \rho | E_0 \rangle}{\langle E_1 | \rho | E_1 \rangle}}. \quad (5)$$

Here E_0 and E_1 are the two energy levels with $E_1 > E_0$.

In many-body systems, it is usually much harder to engineer experimentally a non-thermal state ρ satisfying $\rho_{\text{ed}} = \rho_{\text{therm}}$. Achieving this requires

$$r_n = \frac{E_n - E_{n-1}}{\ln \frac{\langle E_{n-1} | \rho | E_{n-1} \rangle}{\langle E_n | \rho | E_n \rangle}} \quad (6)$$

to be insensitive to n , in which case $k_B T = r_n$ [44, 45]. Engineering this for non-thermal many-body states ρ is often very difficult, since control of individual energy levels is usually not possible. As a result, the work output from coherence from such systems will typically be small. As we will show below, the energy-level structure of an interacting two-mode BEC allows $\rho_{\text{ed}} \approx \rho_{\text{therm}}$ for particular experimentally realisable initial states, hence allowing for work output with a high contribution from coherence.

2.2. System setup

We consider a two-mode BEC with fixed total boson number N . The two modes could be hyperfine spin states or spatial modes [46]. Number states of the system are denoted by $|n, k\rangle$, with n and $k = N - n$ the number of bosons in the two modes respectively. We denote the annihilation operators for the two modes by \hat{a} and \hat{b} , with $\hat{a}|n, k\rangle = \sqrt{n}|n-1, k\rangle$ and $\hat{b}|n, k\rangle = \sqrt{k}|n, k-1\rangle$. The Hamiltonian for the system is ($\hbar \equiv 1$ here and throughout) [35]

$$\begin{aligned}\hat{H} &= \omega_1 \hat{a}^\dagger \hat{a} + \omega_2 \hat{b}^\dagger \hat{b} + \frac{g_{11}}{2} \hat{a}^\dagger \hat{a}^\dagger \hat{a} \hat{a} + \frac{g_{22}}{2} \hat{b}^\dagger \hat{b}^\dagger \hat{b} \hat{b} + g_{12} \hat{a}^\dagger \hat{b}^\dagger \hat{a} \hat{b} + E_0 \\ &\equiv \Delta \hat{a}^\dagger \hat{a} + g \hat{a}^\dagger \hat{a}^\dagger \hat{a} \hat{a}.\end{aligned}\quad (7)$$

Here ω_i is the single-particle energy and g_{ii} the interaction strength for modes $i = 1, 2$. We have also allowed for interactions between the two modes of strength g_{12} , for example if the two modes are spin states. The vacuum energy is E_0 . The operator $\hat{N} = \hat{a}^\dagger \hat{a} + \hat{b}^\dagger \hat{b}$ commutes with \hat{H} and hence the total boson number is conserved. In the second line of equation (7) we replace $\hat{b}^\dagger \hat{b}$ by $\hat{N} - \hat{a}^\dagger \hat{a}$ and define

$$\Delta \equiv \omega_1 - \omega_2 - (N-1)(g_{22} - g_{12}) \quad (8)$$

and

$$g \equiv \frac{g_{11} + g_{22} - 2g_{12}}{2}. \quad (9)$$

We choose $E_0 = -N\omega_2 - N(N-1)g_{22}/2$ so that $\hat{H}|0, N\rangle = 0$ for convenience. The choice of E_0 will not affect the net output of any cyclic process, for example the performance of an engine cycle. The detuning Δ for two spatial modes can be controlled via tuning the trapping potential [47], and for two spin states via tuning of a Zeeman field [48, 49]. As will be discussed below, we require thermal states that have a Gaussian (or approximately Gaussian) distribution over states $|n, N-n\rangle$, which requires $g > 0$. Hence the interaction strengths must satisfy $g_{11} + g_{22} > 2g_{12}$, i.e. the average intramode interaction strength $(g_{11} + g_{22})/2$ must exceed the intermode interaction strength g_{12} . For two spatially separated modes we have $g_{12} = 0$ and therefore $g > 0$ is ensured as long as the intramode interactions g_{ii} are positive, as realised for example in ^{87}Rb and ^{23}Na condensates [50, 51].

Particle conservation confines the system to the subset of states $|n, N-n\rangle$. Since number states are eigenstates of equation (7), the number-state coherence realisable in a two-mode BEC [30] is equivalent to the energy coherence enabling work extraction, equation (3). The thermal state of \hat{H} is,

$$\rho_{\text{therm}} = \frac{1}{Z} e^{-\beta \hat{H}} = \sum_{n=0}^N p_n^{\text{therm}} |n, N-n\rangle \langle n, N-n|, \quad (10)$$

with

$$p_n^{\text{therm}} = \frac{1}{Z} e^{-\beta(gn(n-1) + \Delta n)} \quad (11)$$

the thermal occupation of state $|n, N-n\rangle$ and

$$Z = \sum_{n=0}^N e^{-\beta(gn(n-1) + \Delta n)} \quad (12)$$

the partition function. Due to particle interactions, the boson number distribution of a thermal state is approximately Gaussian when $\beta g > 0$ and $-\beta \Delta \gg \sqrt{\beta g}$, in contrast to the Planck distribution of non-interacting bosons. This feature will be essential for the efficacy of our protocol as it will enable close matching between the initial and thermal boson number distributions. We assume $\beta g \ll 1$; noting that $gN \sim \mu$, where μ is the BEC chemical potential, this is ensured when $\beta \mu / N \ll 1$, a condition satisfied in most realisations of dilute gaseous BECs [52, 53]. We can then approximate the sum in equation (12) by an integral. We also assume $N \gg 1$ and $\langle \hat{a}^\dagger \hat{a} \rangle \ll N$, i.e. most of the particles are in the \hat{b} mode throughout the protocol. We can then set $N \rightarrow \infty$ and approximate $|n, N-n\rangle$ by a harmonic oscillator number state, which simplifies our calculations [54, 55]. Evaluating equation (12) with these two approximations gives

$$Z \approx \sqrt{\frac{\pi}{\beta g}} e^{\beta(g-\Delta)^2/(4g)} \left(\frac{1 + \text{erf}\left(\frac{\beta(g-\Delta)}{2\sqrt{\beta g}}\right)}{2} \right). \quad (13)$$

We denote the $N \rightarrow \infty$ approximation of $|n, N-n\rangle$ by $|n\rangle$ below, however it should be kept in mind that this state is implicitly a two-mode state.

3. Results

Our objective is to find an experimentally realisable density matrix containing coherence in the energy eigenbasis with the same (or almost the same) energy and energy entropy as a thermal state equation (11). As we will now argue, a GCS satisfies these criteria. A GCS is,

$$|\alpha\rangle = \hat{D}(\alpha)|0\rangle = \sum_{n=0}^{\infty} c_n |n\rangle, \quad (14)$$

with $\hat{D}(\alpha) = e^{\alpha\hat{a}^\dagger - \alpha^*\hat{a}}$ the displacement operator and $c_n = e^{-|\alpha|^2/2} \frac{\alpha^n}{\sqrt{n!}}$ [56]. Such a state can be realised via coherent rotation of a pure state $|0, N\rangle$ or $|N, 0\rangle$ [47, 57–61] or via interference measurements [62–64] (see also [65]), and gives rise to phase coherence between the two modes of the BEC [47, 66–70]. Note the upper limit of the sum in equation (14) is set to ∞ by assuming $|\alpha|^2 \ll N$ and $N \gg 1$ (see the discussion above equation (13)). A GCS is a superposition of energy eigenstates of equation (7) and hence $|\alpha\rangle\langle\alpha|$ contains off-diagonal terms $c_m^* c_n |n\rangle\langle m|$ ($m \neq n$); hence a GCS exhibits coherence with respect to the energy eigenbasis. The GCS number-state distribution $p_n^G = |c_n|^2$ is Poissonian with mean and variance equal to $|\alpha|^2$. For large $|\alpha|^2$ we have,

$$p_n^G = \frac{|\alpha|^{2n} e^{-|\alpha|^2}}{n!} \approx \frac{1}{\sqrt{2\pi|\alpha|^2}} e^{-(n-|\alpha|^2)^2/(2|\alpha|^2)}. \quad (15)$$

Choosing

$$|\alpha|^2 = \frac{g - \Delta}{2g}, \quad \beta g = \frac{1}{2|\alpha|^2}, \quad (16)$$

we obtain $p_n^G \approx p_n^{\text{therm}}$, with p_n^{therm} given by equation (11). Equivalently, it is easy to show that equation (6) is independent of n when $|\alpha|^2$ is chosen as in equation (16). Hence with precise tuning of parameters, as given in equation (16), work can be extracted from coherence as discussed in section 2.1.

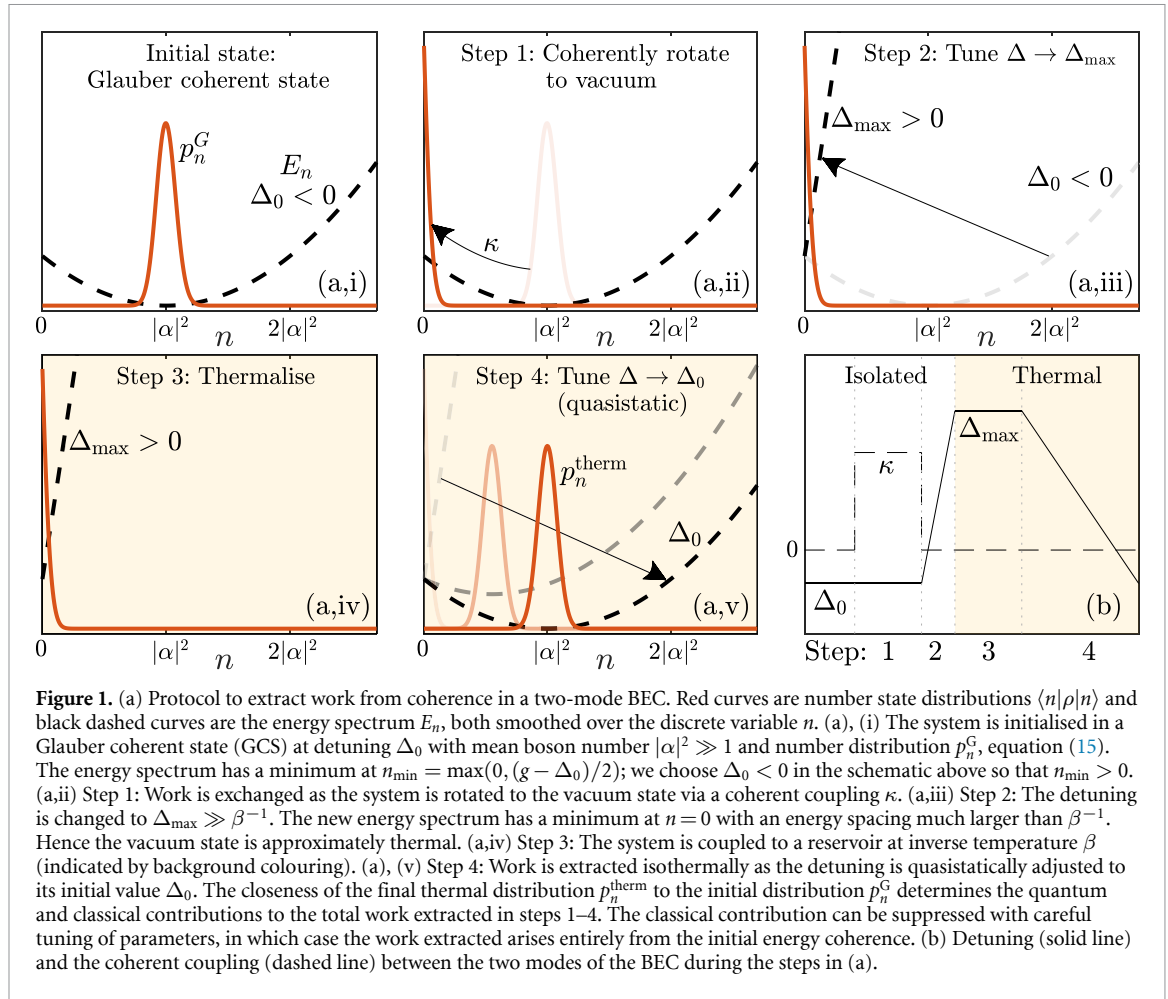
For more general parameters, the work output will have both a contribution from coherence and a ‘classical’ contribution. Below we present an explicit protocol to show how work can be extracted from the coherence of a GCS. We then show how the work output depends on particle number and temperature, identifying a regime where the work output is dominated by the contribution from coherence. Next we show how the work output can be improved by squeezing the initial state and finally we discuss the role of entanglement in the system.

3.1. Protocol to extract work from a GCS

We begin in a GCS, equation (14), with Hamiltonian equation (7) and $\Delta = \Delta_0$. The energy of the initial state is $U_i = \langle\alpha|\hat{H}|\alpha\rangle = \Delta_0|\alpha|^2 + g|\alpha|^4$. To extract work from the GCS we consider the following thermodynamically reversible steps [11] (see figure 1):

1. Coherently couple the two modes of the BEC via the Hamiltonian $\kappa(\hat{b}^\dagger\hat{a} + \hat{a}^\dagger\hat{b})$, with $\kappa > 0$ the coupling rate. Evolve the system so that $|\alpha\rangle$ is displaced to $|0\rangle$ and all particles are in the \hat{b} mode. During this step, coherence is removed and work U_i is exchanged with the coupling field over a time scale κ^{-1} . Turn off the coupling κ so that the system energy is determined by equation (7).
2. Tune the detuning to $\Delta_{\text{max}} > 0$. This does not change the system energy since the system is in state $|0\rangle$.
3. Couple the system to a reservoir at inverse temperature β and allow to thermalise. The detuning Δ_{max} and β are chosen to satisfy $\beta\Delta_{\text{max}} \gg 1$. Occupation of modes $|n\rangle$ with $n > 0$ are therefore thermally suppressed (see equation (12)) and hence $|0\rangle$ is approximately the thermal state. The energy increase during thermalisation is $\approx \Delta_{\text{max}} e^{-\beta\Delta_{\text{max}}}$ and is hence negligible for $\beta\Delta_{\text{max}} \gg 1$.
4. Quasistatically change the detuning back to Δ_0 such that the system remains in thermal equilibrium with the reservoir throughout. Work is extracted and heat is absorbed in this step. The final state is thermal with energy $U_f = -\partial \ln Z / \partial \beta$ evaluated from equation (13) with $\Delta = \Delta_0$.

The coherent coupling in the first step could be achieved using Josephson oscillations for two spatial modes [47, 59] or via a Rabi pulse for two spin states [60, 61]. Complete conversion is possible when κ is much larger than the other energy scales in the problem, which ensures the dynamics is in the Josephson



regime, rather than the self-trapping regime [46, 57, 58, 71]. Note the effect of changing Δ in steps 2–4 could also be achieved by manipulating g using a Feshbach resonance [72–74] with Δ fixed: g would be increased to a value $\beta g_{\max} \gg 1$ in steps 2 and 3 and then quasistatically reduced back to its initial value in step 4. This alternative protocol would not change the results below.

The total mean work output from the protocol in figure 1 is [11]

$$W = U_i - U_f - \beta^{-1} (S_i^V - S_f^V), \quad (17)$$

where S_i^V (S_f^V) are the initial (final) von Neumann entropies of the system.

For the protocol in figure 1 we have $S_i^V = 0$ since the initial state is pure and $S_f^V = S_f^E$ since the final state is thermal. Here S_i^E (S_f^E) are the energy entropies for the initial (final) state. The total entropic change $S_f^V - S_i^V$ can now be decomposed into a classical contribution $S_f^E - S_i^E$ and a quantum contribution $S_i^E - S_i^V = D(\rho||\rho_{\text{ed}})$ arising from coherence, equation (3). The work then consists of two parts [11, 13, 75], a quantum part as defined in equation (4), as well as a classical part:

$$\begin{aligned} W_{\text{quant}} &= \beta^{-1} (S_i^E - S_i^V) \\ W_{\text{class}} &= U_i - U_f - \beta^{-1} (S_f^E - S_i^E). \end{aligned} \quad (18)$$

Note that a projection of the initial state equation (14) onto the energy eigenbasis prior to work extraction, i.e. $\rho \rightarrow \rho_{\text{ed}}$, would result in $W_{\text{quant}} = 0$, but would not change W_{class} . The protocol in figure 1 avoids such projection, allowing W_{quant} to be extracted.

3.2. Classical and quantum contributions to the work extracted from a GCS

With an initial state (14), the outputs W_{quant} and W_{class} in equation (18) can be calculated analytically. We choose $|\alpha|^2$ so that the GCS has mean boson number equal to the thermal state,

$$|\alpha|^2 = \langle \hat{n} \rangle_{\text{therm}} \equiv \langle \hat{n} \rangle. \quad (19)$$

Here $\hat{n} = \hat{a}^\dagger \hat{a}$ and a ‘therm’ subscript denotes expectation values for state ρ_{therm} , equation (10). We have checked that this choice of $|\alpha|$ minimises W_{class} to a very good approximation over the parameters explored. The energetic and entropic terms in equation (18) are

$$\begin{aligned} U_i - U_f &= g(\langle \hat{n} \rangle - \langle \delta \hat{n}^2 \rangle_{\text{therm}}), \\ S_i^E &= \frac{1}{2} + \frac{1}{2} \ln(2\pi \langle \hat{n} \rangle) + O\left(\frac{1}{\langle \hat{n} \rangle}\right), \\ S_f^E &= \frac{1}{2} + \frac{1}{2} \ln(2\pi \langle \delta \hat{n}^2 \rangle_{\text{therm}}) + S_{\text{NG}}, \end{aligned} \quad (20)$$

where $\langle \delta \hat{n}^2 \rangle = \langle \hat{n}^2 \rangle - \langle \hat{n} \rangle^2$. We have also introduced

$$S_{\text{NG}} = \ln \frac{1 + \text{erf} u}{2} - uG(u) - \ln \left[1 - 2uG(u) - 2G(u)^2 \right], \quad (21)$$

with $u = \frac{\beta(g - \Delta_0)}{2\sqrt{\beta g}}$ and $G(u) = \frac{e^{-u^2}}{\sqrt{\pi}(1 + \text{erf} u)} = O(e^{-\beta \Delta_0^2 / (4g)})$. The entropic correction S_{NG} arises since the thermal distribution is not a perfect Gaussian, and is only important for $u \lesssim 1$.

The thermal mean and variance are

$$\langle \hat{n} \rangle_{\text{therm}} = \frac{1}{\sqrt{\beta g}} (u + G(u)), \quad (22)$$

$$\langle \delta \hat{n}^2 \rangle_{\text{therm}} = \frac{1}{2\beta g} (1 - 2uG(u) - 2G(u)^2). \quad (23)$$

Again, the $G(u)$ terms are non-Gaussian corrections, which are only important for $u \lesssim 1$. Note for $u \gg 1$ we have $u^2 \approx \langle \hat{n} \rangle_{\text{therm}}^2 / (2\langle \delta \hat{n}^2 \rangle_{\text{therm}})$, in which case u^{-2} is essentially the normalized second-order correlation function of the thermal bosonic field [76]. The thermal mean, variance and third central moment $\langle \delta \hat{n}^3 \rangle = \langle (\hat{n} - \langle \hat{n} \rangle)^3 \rangle$ are shown in the inset to figure 2(a). We focus on cases $\langle \hat{n} \rangle_{\text{therm}} \gtrsim 1$, which is ensured when the initial detuning is less than the reservoir temperature,

$$-\infty < \beta \Delta_0 \lesssim 1. \quad (24)$$

We hence allow $\beta \Delta_0$ to be negative. This is easy to engineer in a two-mode BEC but difficult to engineer in other bosonic systems that do not have a constrained particle number, e.g. photons.

Analytic expressions for W_{class} and W_{quant} follow from equations (18)–(23) and are plotted in figure 2(a) as a function of $\langle \hat{n} \rangle$. Note $\langle \hat{n} \rangle$ is itself a function of Δ_0 , according to equation (22), and hence varying $\langle \hat{n} \rangle$ corresponds to an implicit variation of Δ_0 . The minimum of the classical work occurs when p_n^G and p_n^{therm} are as close as possible, see figure 2(b). For large $\langle \hat{n} \rangle$ both distributions are approximately Gaussian and hence will be equal when their respective means and variances are equal. Since p_n^G has equal mean and variance, this requires

$$|\alpha|^2 = \langle \hat{n} \rangle_{\text{therm}} = \langle \delta \hat{n}^2 \rangle_{\text{therm}}. \quad (25)$$

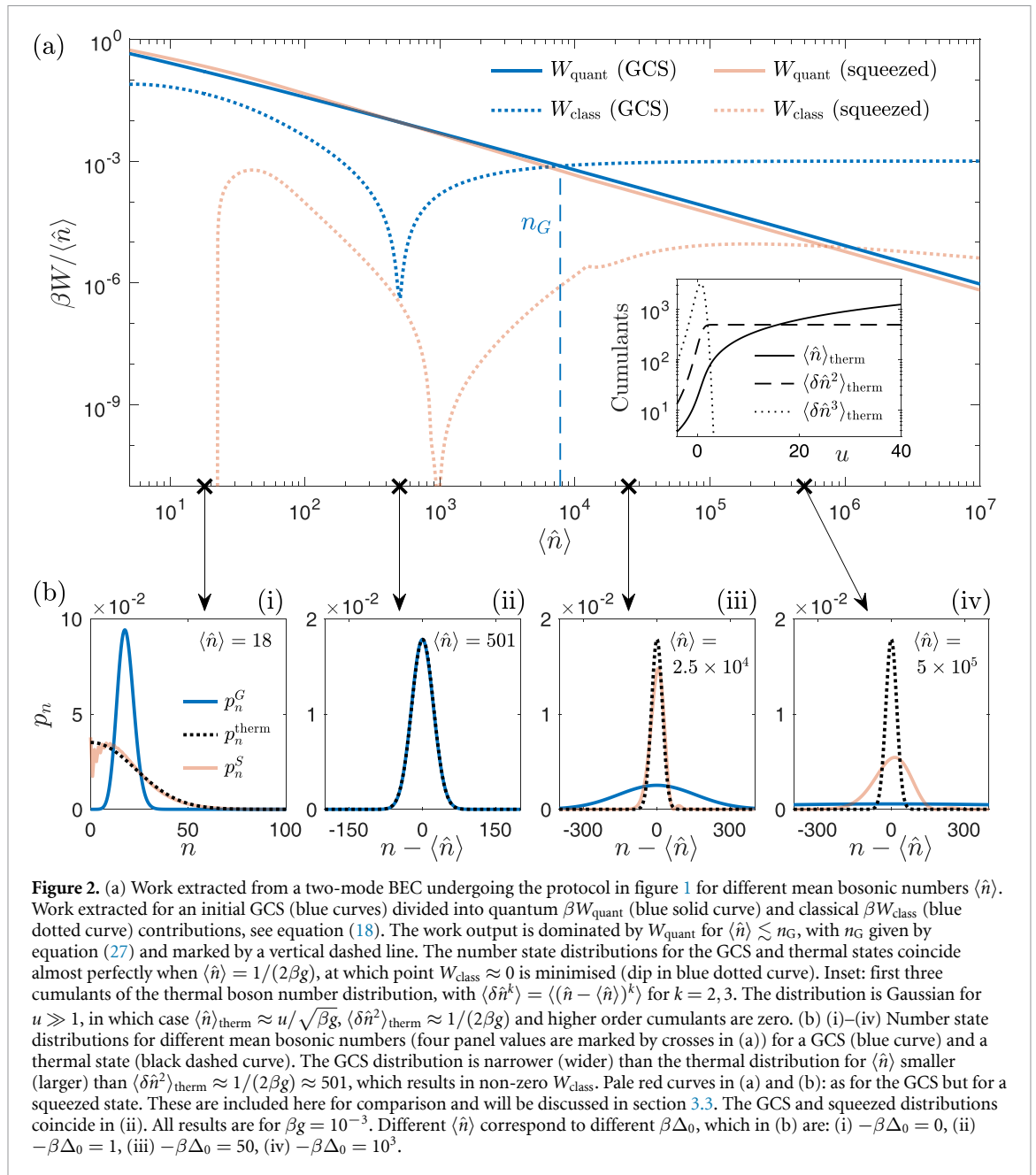
This occurs when $\beta \Delta_0 \approx -1$, at which point $\langle \hat{n} \rangle_{\text{therm}} = \langle \delta \hat{n}^2 \rangle_{\text{therm}} \approx 1/(2\beta g)$. At this optimal point, $W_{\text{class}} = O(\langle \hat{n} \rangle^{-1})$ and the work output almost exclusively consists of W_{quant} . (Note our choice of units: plotting work in units of β^{-1} is equivalent to plotting the information lost if the work was dissipated as heat, according to Landauer’s principle [77].)

For $\langle \hat{n} \rangle \neq \langle \delta \hat{n}^2 \rangle_{\text{therm}}$, the protocol is suboptimal in the sense that W_{class} is no longer approximately zero. Here the thermal bosons are either bunched or anti-bunched, caused by the boson interactions [78]. For $\langle \hat{n} \rangle > \langle \delta \hat{n}^2 \rangle_{\text{therm}}$ (thermal anti-bunching), large number fluctuations in the initial state result in a large $U_i - U_f$, see figure 2(b). In this regime, $u \gg 1$ and equations (20)–(23) simplify to give

$$\begin{aligned} W_{\text{class}} &\approx g\langle \hat{n} \rangle - \frac{1}{2\beta} - \frac{1}{2\beta} \ln(2\beta g \langle \hat{n} \rangle), \\ W_{\text{quant}} &\approx \frac{1}{2\beta} + \frac{1}{2\beta} \ln(2\pi \langle \hat{n} \rangle). \end{aligned} \quad (u \gg 1) \quad (26)$$

Using equation (26), we find that $W_{\text{quant}} > W_{\text{class}}$ for

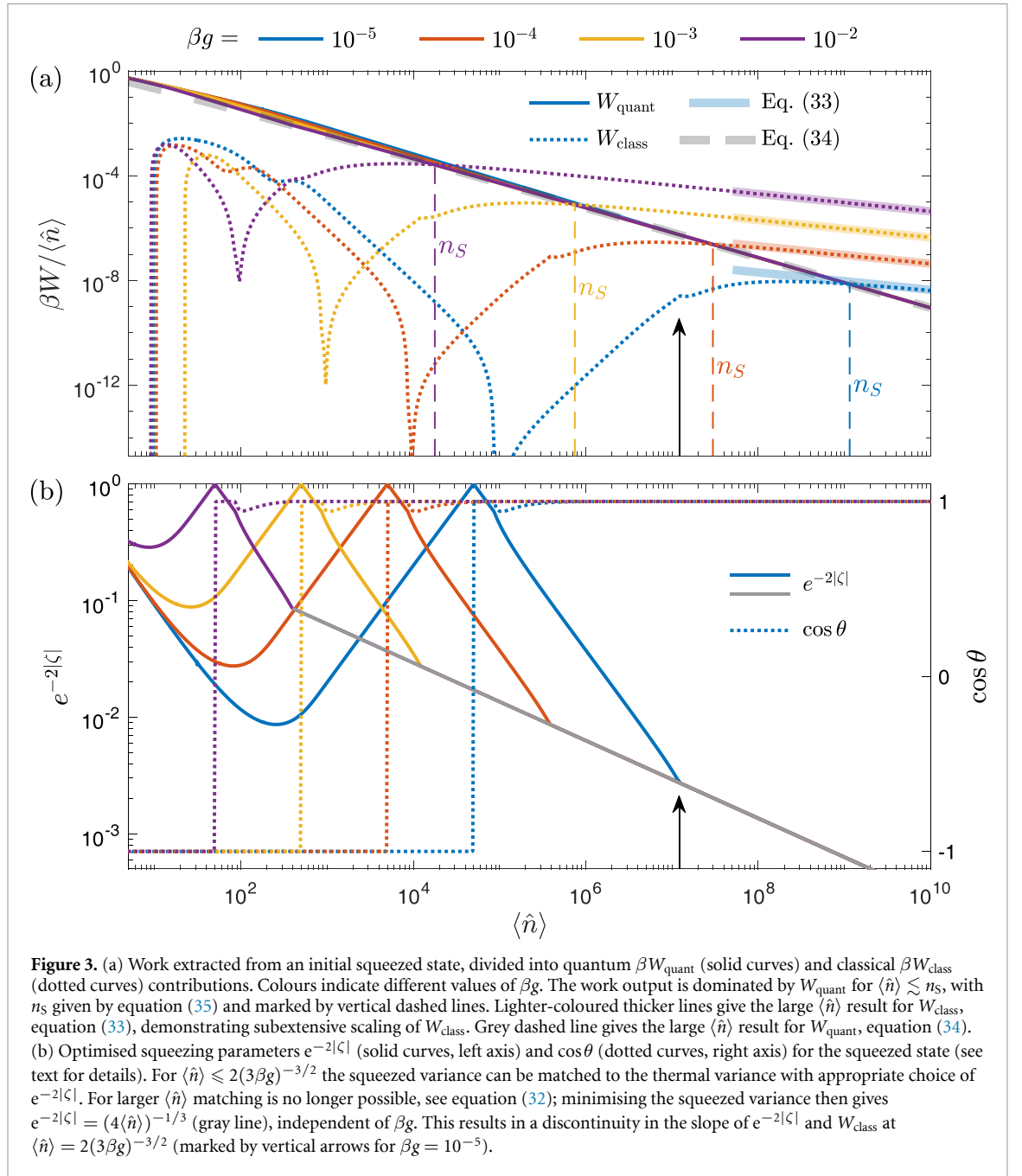
$$\langle \hat{n} \rangle \lesssim \frac{1}{\beta g} \left[-\Omega_{-1} \left(-\sqrt{\frac{\beta g}{4\pi \exp(2)}} \right) \right] \equiv n_G, \quad (27)$$



see figure 2(a). Here Ω_k is the k th branch of the omega function [79]. The function $-\Omega_{-1}(-x)$ satisfies $1 \leq -\Omega_{-1}(-x) < \infty$ for $x \in (0, \exp(-1)]$ and monotonically decreases with increasing x , with $-\Omega_{-1}(-x) \sim \ln(\frac{1}{x} \ln \frac{1}{x})$ for small x [80]. Hence, ignoring logarithmic corrections, n_G decreases with increasing βg as $n_G \sim 1/(\beta g)$. For $\langle \hat{n} \rangle > n_G$, the classical work output grows extensively due to the extensive growth of $U_i - U_f$, see equation (26). The quantum work also increases with $\langle \hat{n} \rangle$ due to increased coherence in the initial state. The increase, however, is subextensive, with $W_{\text{quant}} \sim \frac{1}{2\beta} \ln \langle \hat{n} \rangle$. For $\langle \hat{n} \rangle < \langle \delta \hat{n}^2 \rangle_{\text{therm}}$ (thermal bunching), the number fluctuations of the initial state are less than the final state, see figure 2(b). Although this increases W_{class} , we still have $W_{\text{quant}} > W_{\text{class}}$ as long as $\langle \hat{n} \rangle \gg 1$, see figure 2(a).

3.3. Improved protocol using squeezing

The boson number distribution of a GCS is Poissonian, and hence the mean and variance are always equal. For sufficiently large mean boson number, equation (27), the work output becomes dominated by W_{class} . The classical work output can be suppressed much more effectively by using a squeezed initial state. Squeezing of a two-mode BEC is possible using multiple techniques [35, 81], including time evolution with a one-axis twisting Hamiltonian [33, 82, 83] and parametric downconversion via spin-changing collisions [84–86].



A displaced squeezed state is [87–89],

$$|\alpha, \zeta\rangle = \hat{D}(\alpha) \hat{S}(\zeta) |0\rangle, \quad (28)$$

where $\hat{S}(\zeta) = e^{(\zeta^* \hat{a} \hat{a} - \zeta \hat{a}^\dagger \hat{a}^\dagger)/2}$ is the squeezing operator and $\zeta = |\zeta| e^{i\theta}$ parameterises the squeezing. Without loss of generality we take α to be real. The distribution $p_n^S = |\langle n | \alpha, \zeta \rangle|^2$ is then [90, 91]

$$p_n^S = \frac{\left(\frac{1}{2} \tanh |\zeta|\right)^n}{n! \cosh |\zeta|} |H_n(\lambda \alpha)|^2 e^{-\alpha^2 (1 + \cos \theta \tanh |\zeta|)}, \quad (29)$$

with H_n the Hermite polynomials ($H_0(x) = 1$, $H_1(x) = 2x$, etc) and

$$\lambda = \frac{e^{-i\theta/2} \cosh |\zeta| + e^{i\theta/2} \sinh |\zeta|}{\sqrt{\sinh(2|\zeta|)}}. \quad (30)$$

The boson number distribution for a squeezed state can have a variance smaller or larger than its mean, controllable via the squeezing parameter ζ . This additional control allows the initial number distribution to

be matched more closely to p_n^{therm} , see figure 2(b). The work output from an initial squeezed state is compared with that of a GCS in figure 2(a). Squeezing suppresses W_{class} over a much larger range of $\langle \hat{n} \rangle$ compared to the GCS. Note the small but finite minimum of $W_{\text{class}}/\langle \hat{n} \rangle$ for a GCS, which arises due to the approximation in equation (15), is reduced even further by squeezing, see figure 2(a). Further squeezed results are shown in figure 3(a) for different values of βg . For the squeezed state, we choose $|\alpha|^2$ so that the mean boson number is equal to that of the thermal state and choose ζ to minimise differences in higher order moments. Details are discussed in appendix A and the values of $|\zeta|$ and $\cos\theta$ obtained are plotted in figure 3(b). Numerical details to obtain p_n^S are described in appendix B.

Although squeezing gives much greater control over the initial boson number distribution, its variance is still constrained by $\langle \hat{n} \rangle$ [92]. For large $\langle \hat{n} \rangle$ the minimum variance possible for a squeezed state is (see appendix C)

$$\min\langle \delta \hat{n}^2 \rangle \approx \left(\frac{27}{32}\right)^{1/3} \langle \hat{n} \rangle^{2/3} \quad (31)$$

Achieving $\langle \delta \hat{n}^2 \rangle = \langle \delta \hat{n}^2 \rangle_{\text{therm}}$ is hence only possible when the mean boson number is not too large,

$$\langle \hat{n} \rangle \lesssim \sqrt{\frac{32\langle \delta \hat{n}^2 \rangle_{\text{therm}}^3}{27}} \approx \sqrt{\frac{4}{27(\beta g)^3}}. \quad (32)$$

The constraint (32) should be contrasted with the strict constraint for a GCS, equation (25). Matching the mean and variances of p_n^S and p_n^{therm} gives $U_i = U_f$ and hence $W_{\text{class}} = \beta^{-1}(S_f^E - S_i^E)$, see equation (18).

If the mean boson number is too large such that equation (32) is not satisfied, the variance of the squeezed distribution cannot be made small enough to match $\langle \delta \hat{n}^2 \rangle_{\text{therm}}$. We then choose $\langle \delta \hat{n}^2 \rangle$ to take on its minimum value equation (31) by choosing $e^{-2|\zeta|} = (4\langle \hat{n} \rangle)^{-1/3}$ (see appendix C). This results in subextensive scaling of W_{class} for large $\langle \hat{n} \rangle$,

$$W_{\text{class}} \sim g \left(\frac{27}{32}\right)^{1/3} \langle \hat{n} \rangle^{2/3}, \quad (33)$$

see figure 3(a). Notably, this contrasts the extensive scaling of W_{class} for a GCS, which arises from the strict constraint $\langle \hat{n} \rangle = \langle \delta \hat{n}^2 \rangle$, see figure 2(a) and (26). For large $\langle \hat{n} \rangle$, we find W_{quant} is well approximated by

$$W_{\text{quant}} \approx \frac{1}{2\beta} + \frac{1}{2\beta} \ln \left[2\pi \left(\frac{27}{32}\right)^{1/3} \langle \hat{n} \rangle^{2/3} \right], \quad (34)$$

see figure 3(a). This follows from approximating p_n^S by a Gaussian distribution and using equation (31). Equation (34) and the analogous expression for W_{class} are identical in form to equation (26), but with $\langle \hat{n} \rangle$ replaced by the variance equation (31). This gives the following criteria for $W_{\text{quant}} > W_{\text{class}}$,

$$\langle \hat{n} \rangle \lesssim \sqrt{\frac{32}{27} n_G^3} \equiv n_S, \quad (35)$$

with n_G the equivalent bound for a GCS given by equation (27). The estimate equation (35) agrees well with our numerics, see figure 3(a). Notably, $n_S \gg n_G$ for large n_G .

For small $\langle \hat{n} \rangle$, we observe an abrupt drop in W_{class} , see figure 3(a). At this point, S_i^E increases above S_f^E and hence W_{class} becomes negative ($W_{\text{class}} = S_f^E - S_i^E$ for small $\langle \hat{n} \rangle$, see equation (32)). We expect that the increase in S_i^E above S_f^E is due to oscillations that arise in the squeezed distribution for small $\langle \hat{n} \rangle$ [93, 94], see figure 2(b) [95].

3.4. Relation with entanglement

Finally, we show how the work from coherence in this system can equivalently be interpreted as work from entanglement [96–99]. To see this, we evaluate the entanglement entropy \mathcal{S} between the two modes of the BEC. A sufficient condition for entanglement is then $\mathcal{S} > 0$ [100]. The entanglement entropy of a pure state ρ is

$$\mathcal{S} = -\text{Tr}_1 \rho_1 \log \rho_1, \quad (36)$$

where $\rho_1 = \text{Tr}_2 \rho$ and Tr_i is a partial trace over boson states of modes $i = 1, 2$. The trace Tr_2 can be evaluated in the number state basis for both modes. Due to conservation of total particle number, this projects ρ onto the number state basis for the first mode,

$$\rho_1 = \sum_{n=0}^N \langle n, N-n | \rho | n, N-n \rangle |n\rangle_{11} \langle n| \quad (37)$$

with $|n\rangle_{11} \langle n| = \text{Tr}_2 |n, N-n\rangle \langle n, N-n|$. The ‘1’ subscript distinguishes $|n\rangle_1$ from the implicitly two-mode state $|n\rangle$. Equations (36) and (37) give

$$\mathcal{S} = S_i^E = \beta W_{\text{quant}}. \quad (38)$$

Hence the coherence in this system arises due to entangling correlations between the two modes, which is subsequently extracted as W_{quant} . The final thermal state is a classical mixture of product states, and hence does not possess any entanglement. The quantum work output from coherence can therefore equivalently be interpreted as work from entanglement. Squeezing results in additional entanglement according to the criteria in [32, 101].

4. Discussion and conclusion

We have shown how work can be extracted from coherence in a two-mode BEC. Work almost entirely from coherence can be extracted from a GCS with precisely tuned mean boson number. The protocol can be substantially improved using squeezing, enabling work extraction predominantly from coherence over a much broader range of parameters. Due to the many-body nature of the system, the work from coherence can equivalently be interpreted as work from entanglement.

The coherent steps in our protocol can be realised in current experiments with two-mode BECs, which could be spatial or spin modes [46]. For two spatial modes the detuning can be controlled by varying trap depth [47] and populations can be coherently controlled using Josephson oscillations [47, 59]. For two spin states the detuning can be controlled using Zeeman fields [48, 49] and populations can be controlled using a Rabi pulse [60, 61]. The effect of changing Δ in the protocol could also be achieved by manipulating g using a Feshbach resonance [72–74]. Squeezing of a two-mode BEC can be realised using a variety of techniques [33, 35, 81–86]. Our protocol requires $\beta g \ll 1$, which is satisfied in most realisations of dilute gaseous BECs [52, 53].

The experimentally challenging part of the protocol is the thermalisation of the system with a reservoir (step 3 in figure 1). This could potentially be achieved by immersing the system in a thermal quantum gas of another species, in analogy with sympathetic cooling [102]. An optical tweezer trap would allow the system to be moved in and out of the reservoir as needed. Particle exchange between the two modes during thermalization could occur via tunnelling for two spatial modes [103, 104] or via spin-changing collisions with the reservoir for two spin states [105–108]. We have assumed decoherence only occurs during the thermalising step of our protocol. Additional decoherence will likely reduce the work output by a term that scales linearly with the irreversible entropy production [75].

The Hamiltonian equation (7) also describes a large, fully-connected spin chain [109] and hence could be realised in other atomic systems [35], including atomic ensembles coupled to light [110, 111], Rydberg arrays [112, 113] and trapped ions [114, 115]. The Hamiltonian also resembles that of photons in a non-linear medium [90], with the important difference that we allow the free-photon spectrum to be negative, $\Delta < 0$. To realise this, photon number would need to be conserved [116, 117].

We have limited our analysis to Glauber coherent and squeezed states. Improved operation may be possible using self-phase modulation of the squeezed state [118] or by using non-Gaussian states [119] at the expense of more involved state generation. We have also limited our analysis to initial states with zero von Neumann entropy; relaxing this provides an interesting area for future investigation. Extracting work from coherence can enhance power output compared to classical systems [6]. Our results provide a starting point to explore this in a two-mode BEC, and may result in a many-body quantum advantage when incorporated into an engine cycle.

Data availability statement

The data cannot be made publicly available upon publication because no suitable repository exists for hosting data in this field of study. The data that support the findings of this study are available upon reasonable request from the authors.

Acknowledgments

This research was supported by the Australian Research Council Centre of Excellence for Engineered Quantum Systems (EQUS, CE170100009) and the Australian government Department of Industry, Science, and Resources via the Australia-India Strategic Research Fund (AIRXIV000025). FC and JA gratefully acknowledge funding from the Foundational Questions Institute Fund (FQXi-IAF19-01) and EPSRC (EP/R045577/1). J A thanks the Royal Society for support.

Appendix A. Choosing squeezing parameters

We choose α and ζ for the initial squeezed state as follows. The first three cumulants of p_n^S are evaluated from the generating function $K(s) = \ln \sum_n p_n^S e^{sn}$, which can be written in closed form using Mehler's formula [120]

$$\sum_{n=0}^{\infty} \frac{H_n(x)H_n(y)}{n!} \left(\frac{u}{2}\right)^n = \frac{1}{\sqrt{1-u^2}} e^{\frac{2xyu - (x^2+y^2)u^2}{1-u^2}}. \quad (\text{A1})$$

This gives

$$\begin{aligned} \langle \hat{n} \rangle &= \sinh^2 |\zeta| + |\alpha|^2, \\ \langle \delta \hat{n}^2 \rangle &= 2 \cosh^2 |\zeta| \sinh^2 |\zeta| + |\alpha|^2 [\cosh(2|\zeta|) - \sinh(2|\zeta|) \cos \theta], \\ \langle \delta \hat{n}^3 \rangle &= \cosh(2|\zeta|) \sinh^2(2|\zeta|) + \frac{3|\alpha|^2}{2} \left[\cosh(4|\zeta|) - \frac{1}{3} - \sinh(4|\zeta|) \cos \theta \right], \end{aligned} \quad (\text{A2})$$

with $\langle \delta n^k \rangle = \langle (n - \langle \hat{n} \rangle)^k \rangle$ for $k = 2, 3$. We set $\langle \hat{n} \rangle = \langle \hat{n} \rangle_{\text{therm}}$ by choosing $|\alpha|^2 = \langle \hat{n} \rangle_{\text{therm}} - \sinh^2 |\zeta|$. We solve for $|\zeta|$ by minimising $|\langle \delta n^2 \rangle - \langle \delta \hat{n}^2 \rangle_{\text{therm}}|$. Since the Hamiltonian (7) depends only on $\langle \hat{n} \rangle$ and $\langle \delta \hat{n}^2 \rangle$, this choice minimises $|U_f - U_i|$. Additionally, for not-too-large squeezing this minimises $|S_f^E - S_i^E|$. We then choose $\cos \theta$ to minimise $|\langle \delta n^3 \rangle|$.

Appendix B. Numerical details for extracting squeezed state statistics

Numerical computation of p_n^S requires care for large n due to numerical overflow and underflow [121]. We evaluate p_n^S using the underlying recursion relation [90, 91] $c_n = \langle n | \alpha, \zeta \rangle = \frac{\alpha(1+e^{i\theta} \tanh |\zeta|)}{\sqrt{n}} c_{n-1} - e^{i\theta} \tanh |\zeta| \sqrt{\frac{n-1}{n}} c_{n-2}$. After each iteration we normalise the distribution. Defining $\Delta n = \text{ceil}(50\sqrt{\langle \delta \hat{n}^2 \rangle})$, we begin the recursion at $n^* = \max(0, \text{round}(\langle \hat{n} \rangle - \Delta n/2))$ with $c_{n^*} = 1$ and $c_{n < n^*} = 0$, and evaluate terms up to $n^* + \Delta n$. In cases where $n^* > 0$, we find $|\alpha| \gg 1$ and hence $c_{n^*+1} \approx \frac{\alpha(1+e^{i\theta} \tanh |\zeta|)}{\sqrt{n^*}} c_{n^*}$ (this is exact for $n^* = 0$). Hence why the values of $c_{n < n^*}$ are not needed.

Appendix C. Minimum variance of a squeezed state

To a very good approximation $\cos \theta = \pm 1$, see figure 3(b). Defining $x = e^{2|\zeta| \cos \theta}$ ($= e^{\pm 2|\zeta|}$), the equation for $\langle \delta \hat{n}^2 \rangle$ is (see equation (A2)),

$$\langle \delta \hat{n}^2 \rangle = \frac{1}{8x^2} \left(x^4 - 4x^2 + 8 \left(\langle \hat{n} \rangle + \frac{1}{2} \right) x - 1 \right). \quad (\text{C1})$$

Stationary points of $d\langle \delta \hat{n}^2 \rangle / dx$ satisfy the polynomial

$$x^4 - 4 \left(\langle \hat{n} \rangle + \frac{1}{2} \right) x + 1 = 0. \quad (\text{C2})$$

Equation (C2) can be solved for x using standard methods. For large $\langle \hat{n} \rangle$ this gives two real roots and two complex roots. The two real roots are

$$\begin{aligned}
 x_1 &\approx \frac{1}{4\langle \hat{n} \rangle + 2}, \\
 x_2 &\approx (4\langle \hat{n} \rangle)^{1/3},
 \end{aligned}
 \tag{C3}$$

with x_1 corresponding to a local maximum of equation (C1) and $x_2 > x_1$ a local minimum. Substituting $x \leq x_1$ into the expression for $\langle \hat{n} \rangle$ (equation (A2)) would give a negative value for $|\alpha|^2$, hence $x > x_1$. Therefore x_2 gives the global minimum of $\langle \delta \hat{n}^2 \rangle$ for valid values of x . Substituting x_2 into equation (C1) gives equation (31) for large $\langle \hat{n} \rangle$.

ORCID iDs

L A Williamson  <https://orcid.org/0000-0003-3487-1528>

F Cerisola  <https://orcid.org/0000-0003-2961-739X>

J Anders  <https://orcid.org/0000-0002-9791-0363>

Matthew J Davis  <https://orcid.org/0000-0001-8337-0784>

References

- [1] Åberg J, 2006 Quantifying superposition (arXiv: [quant-ph/0612146](https://arxiv.org/abs/quant-ph/0612146))
- [2] Streltsov A, Adesso G and Plenio M B 2017 Colloquium: Quantum coherence as a resource *Rev. Mod. Phys.* **89** 041003
- [3] Vinjanampathy S and Anders J 2016 Quantum thermodynamics *Contemp. Phys.* **57** 545
- [4] Goold J, Huber M, Riera A, Del Rio L and Skrzypczyk P 2016 The role of quantum information in thermodynamics—a topical review *J. Phys. A: Math. Theor.* **49** 143001
- [5] Binder F, Correa L A, Gogolin C, Anders J and Adesso G (eds) 2018 *Thermodynamics in the Quantum Regime — Fundamental Aspects and New Directions* (Springer Nature)
- [6] Uzdin R, Levy A and Kosloff R 2015 Equivalence of quantum heat machines and quantum-thermodynamic signatures *Phys. Rev. X* **5** 031044
- [7] Uzdin R 2016 Coherence-induced reversibility and collective operation of quantum heat machines via coherence recycling *Phys. Rev. Appl.* **6** 024004
- [8] Klatzow J, Becker J N, Ledingham P M, Weinzetl C, Kaczmarek K T, Saunders D J, Nunn J, Walmsley I A, Uzdin R and Poem E 2019 Experimental demonstration of quantum effects in the operation of microscopic heat engines *Phys. Rev. Lett.* **122** 110601
- [9] Horodecki M and Oppenheim J 2013 Fundamental limitations for quantum and nanoscale thermodynamics *Nat. Commun.* **4** 2059
- [10] Scully M O, Zubairy M S, Agarwal G S and Walther H 2003 Extracting work from a single heat bath via vanishing quantum coherence *Science* **299** 862
- [11] Kammerlander P and Anders J 2016 Coherence and measurement in quantum thermodynamics *Sci. Rep.* **6** 22174
- [12] Korzekwa K, Lostaglio M, Oppenheim J and Jennings D 2016 The extraction of work from quantum coherence *New J. Phys.* **18** 023045
- [13] Francica G, Binder F C, Guarnieri G, Mitchison M T, Goold J and Plastina F 2020 Quantum coherence and ergotropy *Phys. Rev. Lett.* **125** 180603
- [14] Brandão F G S L, Horodecki M, Oppenheim J, Renes J M and Spekkens R W 2013 Resource theory of quantum states out of thermal equilibrium *Phys. Rev. Lett.* **111** 250404
- [15] Chitambar E and Gour G 2019 Quantum resource theories *Rev. Mod. Phys.* **91** 025001
- [16] Ciampini M A, Mancino L, Orioux A, Vigliar C, Mataloni P, Paternostro M and Barbieri M 2017 Experimental extractable work-based multipartite separability criteria *Quantum Inf.* **3** 10
- [17] Millen J and Xuereb A 2016 Perspective on quantum thermodynamics *New J. Phys.* **18** 011002
- [18] Cangemi L M, Bhadra C and Levy A 2023 Quantum engines and refrigerators *Phys. Rep.* **1087** 1–71
- [19] Bloch I, Dalibard J and Nascimbène S 2012 Quantum simulations with ultracold quantum gases *Nat. Phys.* **8** 267
- [20] Langen T, Geiger R and Schmiedmayer J 2015 Ultracold atoms out of equilibrium *Annu. Rev. Condens. Matter Phys.* **6** 201
- [21] Myers N M, Peña F J, Negrete O, Vargas P, De Chiara G and Deffner S 2022 Boosting engine performance with Bose–Einstein condensation *New J. Phys.* **24** 025001
- [22] Jaramillo J, Beau M and del Campo A 2016 Quantum supremacy of many-particle thermal machines *New J. Phys.* **18** 075019
- [23] Fogarty T and Busch T 2020 A many-body heat engine at criticality *Quantum Sci. Technol.* **6** 015003
- [24] Simmons E Q, Sajjad R, Keithley K, Mas H, Tanlimco J L, Nolasco-Martinez E, Bai Y, Fredrickson G H and Weld D M 2023 Thermodynamic engine with a quantum degenerate working fluid *Phys. Rev. Res.* **5** L042009
- [25] Koch J, Menon K, Cuestas E, Barbosa S, Lutz E, Fogarty T, Busch T and Widera A 2023 A quantum engine in the BEC–BCS crossover *Nature* **621** 723
- [26] Bengtsson J, Tengstrand M N, Wacker A, Samuelsson P, Ueda M, Linke H and Reimann S M 2018 Quantum Szilard engine with attractively interacting bosons *Phys. Rev. Lett.* **120** 100601
- [27] Boubakour M, Fogarty T and Busch T 2023 Interaction-enhanced quantum heat engine *Phys. Rev. Res.* **5** 013088
- [28] Chen Y-Y, Watanabe G, Yu Y-C, Guan X-W and del Campo A 2019 An interaction-driven many-particle quantum heat engine and its universal behavior *npj Quantum Inf.* **5** 88
- [29] Watson R and Kheruntsyan K, 2023 An interaction-driven quantum many-body engine enabled by atom-atom correlations (arXiv:2308.05266)
- [30] Jo G-B, Shin Y, Will S, Pasquini T A, Saba M, Ketterle W, Pritchard D E, Vengalattore M and Prentiss M 2007 Long phase coherence time and number squeezing of two Bose–Einstein condensates on an atom chip *Phys. Rev. Lett.* **98** 030407
- [31] Orzel C, Tuchman A, Fenselau M, Yasuda M and Kasevich M 2001 Squeezed states in a Bose–Einstein condensate *Science* **291** 2386

- [32] Sørensen A, Duan L-M, Cirac J I and Zoller P 2001 Many-particle entanglement with Bose–Einstein condensates *Nature* **409** 63
- [33] Estève J, Gross C, Weller A, Giovanazzi S and Oberthaler M K 2008 Squeezing and entanglement in a Bose–Einstein condensate *Nature* **455** 1216
- [34] Muessel W, Strobel H, Linnemann D, Hume D B and Oberthaler M K 2014 Scalable spin squeezing for quantum-enhanced magnetometry with Bose-Einstein condensates *Phys. Rev. Lett.* **113** 103004
- [35] Pezzè L, Smerzi A, Oberthaler M K, Schmied R and Treutlein P 2018 Quantum metrology with nonclassical states of atomic ensembles *Rev. Mod. Phys.* **90** 035005
- [36] Szigeti S S, Nolan S P, Close J D and Haine S A 2020 High-precision quantum-enhanced gravimetry with a Bose-Einstein condensate *Phys. Rev. Lett.* **125** 100402
- [37] Polkovnikov A 2011 Microscopic diagonal entropy and its connection to basic thermodynamic relations *Ann. Phys.* **326** 486
- [38] Santos L F, Polkovnikov A and Rigol M 2011 Entropy of isolated quantum systems after a quench *Phys. Rev. Lett.* **107** 040601
- [39] Pusz W and Woronowicz S L 1978 Passive states and KMS states for general quantum systems *Commun. Math. Phys.* **58** 273
- [40] Kosloff R and Rezek Y 2017 The quantum harmonic Otto cycle *Entropy* **19** 136
- [41] Balian R 1989 Gain of information in a quantum measurement *Eur. J. Phys.* **10** 208
- [42] Esposito M and Van den Broeck C 2011 Second law and Landauer principle far from equilibrium *Europhys. Lett.* **95** 40004
- [43] Baumgratz T, Cramer M and Plenio M B 2014 Quantifying coherence *Phys. Rev. Lett.* **113** 140401
- [44] Quan H T, Liu Y-x, Sun C P and Nori F 2007 Quantum thermodynamic cycles and quantum heat engines *Phys. Rev. E* **76** 031105
- [45] Plastina F, Aleccia A, Apollaro T J G, Falcone G, Francica G, Galve F, Lo Gullo N and Zambrini R 2014 Irreversible work and inner friction in quantum thermodynamic processes *Phys. Rev. Lett.* **113** 260601
- [46] Leggett A J 2001 Bose-Einstein condensation in the alkali gases: some fundamental concepts *Rev. Mod. Phys.* **73** 307
- [47] Albiez M, Gati R, Fölling J, Hunsmann S, Cristiani M and Oberthaler M K 2005 Direct observation of tunneling and nonlinear self-trapping in a single bosonic Josephson junction *Phys. Rev. Lett.* **95** 010402
- [48] Matthews M R, Hall D S, Jin D S, Ensher J R, Wieman C E, Cornell E A, Dalfovo F, Minniti C and Stringari S 1998 Dynamical response of a Bose-Einstein condensate to a discontinuous change in internal state *Phys. Rev. Lett.* **81** 243
- [49] Hall D S, Ensher J R, Jin D S, Matthews M R, Wieman C E and Cornell E A 1998 Recent experiments with Bose-condensed gases at JILA, methods for ultrasensitive detection *Proc. SPIE* **3270** 98–106
- [50] Anderson M H, Ensher J R, Matthews M R, Wieman C E and Cornell E A 1995 Observation of Bose-Einstein condensation in a dilute atomic vapor *Science* **269** 198
- [51] Davis K B, Mewes M O, Andrews M R, van Druten N J, Durfee D S, Kurn D M and Ketterle W 1995 Bose-Einstein condensation in a gas of sodium atoms *Phys. Rev. Lett.* **75** 3969
- [52] Ketterle W, Durfee D S and Stamper-Kurn D M 1999 Making, probing and understanding Bose-Einstein condensates *Bose-Einstein Condensation in Atomic Gases, (Series Proc. Int. School of Physics ‘Enrico Fermi’)*, vol 140 (IOS Press) pp 67–176
- [53] Dalfovo F, Giorgini S, Pitaevskii L P and Stringari S 1999 Theory of Bose-Einstein condensation in trapped gases *Rev. Mod. Phys.* **71** 463
- [54] Radcliffe J 1971 Some properties of coherent spin states *J. Phys. A: Gen. Phys.* **4** 313
- [55] Holstein T and Primakoff H 1940 Field dependence of the intrinsic domain magnetization of a ferromagnet *Phys. Rev.* **58** 1098
- [56] Glauber R J 1963a Coherent and incoherent states of the radiation field *Phys. Rev.* **131** 2766
- [57] Millburn G J, Corney J, Wright E M and Walls D F 1997 Quantum dynamics of an atomic Bose-Einstein condensate in a double-well potential *Phys. Rev. A* **55** 4318
- [58] Raghavan S, Smerzi A, Fantoni S and Shenoy S R 1999 Coherent oscillations between two weakly coupled Bose-Einstein condensates: Josephson effects, π oscillations and macroscopic quantum self-trapping *Phys. Rev. A* **59** 620
- [59] Gati R and Oberthaler M K 2007 A bosonic Josephson junction *J. Phys. B: At. Mol. Opt. Phys.* **40** R61
- [60] Matthews M R, Anderson B P, Haljan P C, Hall D S, Holland M J, Williams J E, Wieman C E and Cornell E A 1999 Watching a superfluid untwist itself: recurrence of Rabi oscillations in a Bose-Einstein condensate *Phys. Rev. Lett.* **83** 3358
- [61] Zibold T, Nicklas E, Gross C and Oberthaler M K 2010 Classical bifurcation at the transition from Rabi to Josephson dynamics *Phys. Rev. Lett.* **105** 204101
- [62] Javanainen J and Yoo S M 1996 Quantum phase of a Bose-Einstein condensate with an arbitrary number of atoms *Phys. Rev. Lett.* **76** 161
- [63] Cirac J I, Gardiner C W, Naraschewski M and Zoller P 1996 Continuous observation of interference fringes from Bose condensates *Phys. Rev. A* **54** R3714
- [64] Castin Y and Dalibard J 1997 Relative phase of two Bose-Einstein condensates *Phys. Rev. A* **55** 4330
- [65] Barnett S, Burnett K and Vaccaro J 1996 Why a condensate can be thought of as having a definite phase *J. Res. Natl Inst. Stand. Technol.* **101** 593
- [66] Andrews M, Townsend C, Miesner H-J, Durfee D, Kurn D and Ketterle W 1997 Observation of interference between two Bose condensates *Science* **275** 637
- [67] Hall D S, Matthews M R, Wieman C E and Cornell E A 1998b Measurements of relative phase in two-component Bose-Einstein condensates *Phys. Rev. Lett.* **81** 1543
- [68] Kasevich M A 2002 Coherence with atoms *Science* **298** 1363
- [69] Carruthers P and Nieto M M 1965 Coherent states and the number-phase uncertainty relation *Phys. Rev. Lett.* **14** 387
- [70] Buřiek V, Wilson-Gordon A D, Knight P L and Lai W K 1992 Coherent states in a finite-dimensional basis: their phase properties and relationship to coherent states of light *Phys. Rev. A* **45** 8079
- [71] Simon L and Strunz W T 2012 Analytical results for Josephson dynamics of ultracold bosons *Phys. Rev. A* **86** 053625
- [72] Papp S B, Pino J M and Wieman C E 2008 Tunable miscibility in a dual-species Bose-Einstein condensate *Phys. Rev. Lett.* **101** 040402
- [73] Tojo S, Taguchi Y, Masuyama Y, Hayashi T, Saito H and Hirano T 2010 Controlling phase separation of binary Bose-Einstein condensates via mixed-spin-channel Feshbach resonance *Phys. Rev. A* **82** 033609
- [74] Chin C, Grimm R, Julienne P and Tiesinga E 2010 Feshbach resonances in ultracold gases *Rev. Mod. Phys.* **82** 1225
- [75] Mohammady M, Auffèves A and Anders J 2020 Energetic footprints of irreversibility in the quantum regime *Commun. Phys.* **3** 89
- [76] Glauber R J 1963b The quantum theory of optical coherence *Phys. Rev.* **130** 2529
- [77] Landauer R 1961 Irreversibility and heat generation in the computing process *IBM J. Res. Dev.* **5** 183
- [78] Yang S and John S 2011 Coherence and antibunching in a trapped interacting Bose-Einstein condensate *Phys. Rev. B* **84** 024515
- [79] Also known as the Lambert W -function, denoted by W_k . We avoid this notation to avoid confusion with work output.
- [80] Corless R M, Gonnet G H, Hare D E, Jeffrey D J and Knuth D E 1996 On the Lambert W function *Adv. Comput. Math.* **5** 329

- [81] Ma J, Wang X, Sun C-P and Nori F 2011 Quantum spin squeezing *Phys. Rep.* **509** 89
- [82] Kitagawa M and Ueda M 1993 Squeezed spin states *Phys. Rev. A* **47** 5138
- [83] Wang X and Sanders B C 2003 Relations between bosonic quadrature squeezing and atomic spin squeezing *Phys. Rev. A* **68** 033821
- [84] Duan L-M, Sørensen A, Cirac J I and Zoller P 2000 Squeezing and entanglement of atomic beams *Phys. Rev. Lett.* **85** 3991
- [85] Pu H and Meystre P 2000 Creating macroscopic atomic Einstein-Podolsky-Rosen states from Bose-Einstein condensates *Phys. Rev. Lett.* **85** 3987
- [86] Gross C, Strobel H, Nicklas E, Zibold T, Bar-Gill N, Kurizki G and Oberthaler M K 2011 Atomic homodyne detection of continuous-variable entangled twin-atom states *Nature* **480** 219
- [87] Stoler D 1970 Equivalence classes of minimum uncertainty packets *Phys. Rev. D* **1** 3217
- [88] Yuen H P 1976 Two-photon coherent states of the radiation field *Phys. Rev. A* **13** 2226
- [89] Caves C M 1981 Quantum-mechanical noise in an interferometer *Phys. Rev. D* **23** 1693
- [90] Gerry C C and Knight P L 2005 *Introductory Quantum Optics* (Cambridge University Press)
- [91] Gong J J and Aravind P K 1990 Expansion coefficients of a squeezed coherent state in the number state basis *Am. J. Phys.* **58** 1003
- [92] Bondurant R S and Shapiro J H 1984 Squeezed states in phase-sensing interferometers *Phys. Rev. D* **30** 2548
- [93] Schleich W and Wheeler J 1987a Oscillations in photon distribution of squeezed states and interference in phase space *Nature* **326** 574
- [94] Schleich W and Wheeler J 1987b Oscillations in photon distribution of squeezed states *J. Opt. Soc. Am. B* **4** 1715
- [95] The change of sign of W_{class} means that there is value of $\langle \hat{n} \rangle$ where $W_{\text{class}} = 0$ despite differences in the squeezed and thermal distributions. The choice of squeezing parameters can possibly be optimised to find similar ‘serendipitous’ points of zero or small W_{class} for other values of $\langle \hat{n} \rangle$.
- [96] Perarnau-Llobet M, Hovhannisyan K V, Huber M, Skrzypczyk P, Brunner N and Acín A 2015 Extractable work from correlations *Phys. Rev. X* **5** 041011
- [97] Sapienza F, Cerisola F and Roncaglia A J 2019 Correlations as a resource in quantum thermodynamics *Nat. Commun.* **10** 2492
- [98] Touil A, Çakmak B and Deffner S 2021 Ergotropy from quantum and classical correlations *J. Phys. A: Math. Theor.* **55** 025301
- [99] Francica G, Goold J, Plastina F and Paternostro M 2017 Daemonic ergotropy: enhanced work extraction from quantum correlations *npj Quantum Inf.* **3** 12
- [100] Bennett C H, Bernstein H J, Popescu S and Schumacher B 1996 Concentrating partial entanglement by local operations *Phys. Rev. A* **53** 2046
- [101] Sørensen A S and Mølmer K 2001 Entanglement and extreme spin squeezing *Phys. Rev. Lett.* **86** 4431
- [102] Modugno G, Ferrari G, Roati G, Brecha R J, Simoni A and Inguscio M 2001 Bose-Einstein condensation of potassium atoms by sympathetic cooling *Science* **294** 1320
- [103] Grabert H and Weiss U 1985 Quantum tunneling rates for asymmetric double-well systems with Ohmic dissipation *Phys. Rev. Lett.* **54** 1605
- [104] Fisher M P A and Dorsey A T 1985 Dissipative quantum tunneling in a biased double-well system at finite temperatures *Phys. Rev. Lett.* **54** 1609
- [105] Bradley A S and Blakie P B 2014 Stochastic projected Gross-Pitaevskii equation for spinor and multicomponent condensates *Phys. Rev. A* **90** 023631
- [106] Kawaguchi Y and Ueda M 2012 Spinor Bose-Einstein condensates *Phys. Rep.* **520** 253
- [107] Stamper-Kurn D M and Ueda M 2013 Spinor Bose gases: symmetries, magnetism and quantum dynamics *Rev. Mod. Phys.* **85** 1191
- [108] Bouton Q, Nettersheim J, Burgardt S, Adam D, Lutz E and Widera A 2021 A quantum heat engine driven by atomic collisions *Nat. Commun.* **12** 2063
- [109] Ulyanov V V and Zaslavskii O B 1992 New methods in the theory of quantum spin systems *Phys. Rep.* **216** 179
- [110] Hammerer K, Sørensen A S and Polzik E S 2010 Quantum interface between light and atomic ensembles *Rev. Mod. Phys.* **82** 1041
- [111] Leroux I D, Schleier-Smith M H and Vuletic V 2010 Implementation of cavity squeezing of a collective atomic spin *Phys. Rev. Lett.* **104** 073602
- [112] Bouchoule I and Mølmer K 2002 Spin squeezing of atoms by the dipole interaction in virtually excited Rydberg states *Phys. Rev. A* **65** 041803
- [113] Saffman M, Walker T G and Mølmer K 2010 Quantum information with Rydberg atoms *Rev. Mod. Phys.* **82** 2313
- [114] Sørensen A and Mølmer K 2000 Entanglement and quantum computation with ions in thermal motion *Phys. Rev. A* **62** 022311
- [115] Meyer V, Rowe M A, Kielpinski D, Sackett C A, Itano W M, Monroe C and Wineland D J 2001 Experimental demonstration of entanglement-enhanced rotation angle estimation using trapped ions *Phys. Rev. Lett.* **86** 5870
- [116] Klaers J, Vewinger F and Weitz M 2010a Thermalization of a two-dimensional photonic gas in a ‘white wall’ photon box *Nature Phys.* **6** 512
- [117] Klaers J, Schmitt J, Vewinger F and Weitz M 2010b Bose-Einstein condensation of photons in an optical microcavity *Nature* **468** 545
- [118] Kitagawa M and Yamamoto Y 1986 Number-phase minimum-uncertainty state with reduced number uncertainty in a Kerr nonlinear interferometer *Phys. Rev. A* **34** 3974
- [119] Walschaers M 2021 Non-Gaussian quantum states and where to find them *PRX Quantum* **2** 030204
- [120] Erdélyi A 1953 *Higher Transcendental Functions* vol II
- [121] Bunck B F 2009 A fast algorithm for evaluation of normalized Hermite functions *Bit Numer. Math.* **49** 281